Design of a new five-link haptic device considering its dynamics

Chanwoo Moon, Sungho Lee and J.K. Chung

Precision machinery Research Center, Korea Electronics Technology Institute
Yakdae Dong 192, Wonmi Gu, Puchon Si, Kyunggi Do, Korea
(Tel : +82-32-621-2846; E-mail: mcwnt@keti.re.kr)

Abstract: The haptic system becomes an essential device in the area of tele-operation, video entertainment and medical operation. To control a haptic device, impedance control method is widely used, but force sensor costs so much that open-loop control method is usually preferred for commercial purpose. In this case, modeled/un-modeled dynamics affects the performance of device. In this paper, we present a new 3DOF five-link type haptic device that we can reduce the effect of device dynamics and compensate its dynamics. We also evaluate its performance.

Keywords: Haptic, dynamics, performance, five-link

1. INTRODUCTION

The haptic system which displays force and tactile impression of material becomes an essential device in the area of tele-operation, video entertainment and medical operation. Research areas of haptic system include application study of haptic device, haptic rendering and design of haptic device. Tele-operation is main application area of haptic device. Anderson proposed passivity condition of time delayed tele-operation system[1]. Hong used haptic system to control a remote vehicle and it was devised to generate artificial force to avoid obstacle[2]. Chang designed a wearable haptic device to control a humanoid robot[3]. Currently, haptic device extended its application area to micro manipulation. Sitti manipulated micro scale object with Phantom haptic device and AFM[4]. Recent issue of haptic rendering is modeling method of soft material. Frank used FEM and FPGA hardware to simulate soft material[5]. Kim modeled a 3D object and used a hierarchical approach to reduce computational burden [6], and Unger practiced a peg-in-hole in real and virtual world with his own virtual model[7].

Haptic device must be designed on ergonomics and always guarantee sufficient stability. Its inertia, friction and mass must have minimum effect on its performance. To control haptic device, impedance control method is widely used, but force sensor costs so much that open-loop control method is preferred for commercial purpose. In this case, modeled/un-modeled dynamics affects the performance of device and appears as a parasitic force. There were some trials to compensate the effect of dynamics. Kwon compensated friction force and compared open loop with closed loop haptic control [8].

Here, we design a new 3 DOF five-link type haptic device which has simple dynamics so that we can reduce and compensate the effect of device dynamics. We propose dynamic compensation method and evaluate its performance with some indices.

The organization is as follows. In Section 2, we present a newly designed haptic device and drive dynamics equation. Then, we build a compensator in Section 3. In Section 4, we present some numerical and experimental result, and finally, conclusions are presented in Section 5.

2. HAPTIC DEVICE DESIGN

2.1 Design of haptic mechanism

Commercial haptic device without force sensor is affected by system dynamics and it appears as unexpected force to an operator. To reduce the effect of system dynamics, light weight material is used to implement a haptic device, but it limits their output force, stiffness and price competitiveness.

Parallel mechanism has good output force, but small workspace, while serial mechanism has small output force and large workspace. In this paper we adopt five-link mechanism to get a large workspace and actuate it with three 150W motors to produce sufficient force. As motor power increases, the effect of mass of motor to system dynamics also increases. To minimize un-modeled dynamics which comes from motor and harness, we locate all motors on frame, and actuator torque is transferred by wire and wheel as proposed by Burn[9]. Then modeled dynamics which comes from links structure becomes dominant. Conceptual design of proposed haptic device is shown in Fig. 1 and schematic diagram is shown in Fig. 2.

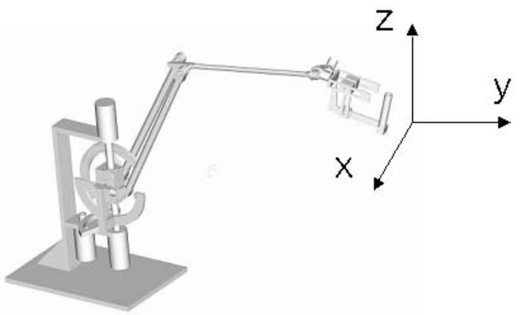

Fig. 1 Conceptual design of proposed haptic device

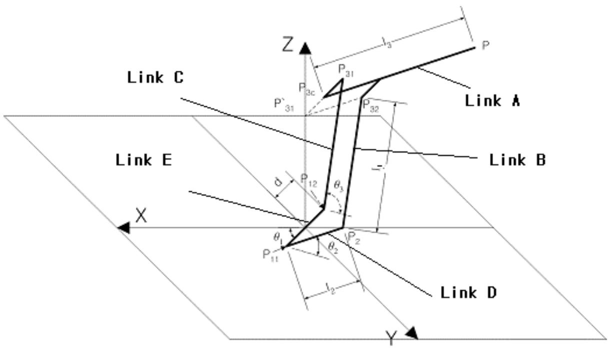

Fig. 2 Schematic diagram of proposed haptic device

2.2 Dynamics of proposed haptic device

Dynamics equation of proposed haptic device is given in the form of equation (1).

$$M\ddot{\theta} + C\dot{\theta} + N + \tau_{friction} = \tau \qquad (1)$$

M : inertia matrix

$$M = \begin{pmatrix} M_{11} & M_{12} & M_{13} \\ M_{21} & M_{22} & M_{23} \\ M_{31} & M_{32} & M_{33} \end{pmatrix}$$

C : Coriolis matrix

$$C = \begin{pmatrix} C_{11} & C_{12} & C_{13} \\ C_{21} & C_{22} & C_{23} \\ C_{31} & C_{32} & C_{33} \end{pmatrix}$$

N : gravity vector

$$N = \begin{pmatrix} N_1 \\ N_2 \\ N_3 \end{pmatrix}$$

Parameters of each links are notated as follows.

Link A:
- L_3: link length
- L_{ac} : length of center of mass including gripper
- M_G : mass of gripper
- M_{Ar} : mass of link
- M_A : $M_G + M_{Ar}$

Link B:
- L_1: link length
- L_{bc} : length of center of mass
- M_B : mass of link

Link C: (link length is same with Link B)
- L_{cc} : length of center of mass including counter balance
- M_{BC} : mass of counter balance
- M_{Cr} : mass of link
- M_C : $M_{BC} + M_{Cr}$

Link D:
- L_2: link length
- L_{dc} : length of center of mass including counter balance
- M_{BD} : mass of gripper
- M_{Dr} : mass of link
- M_D : $M_{BD} + M_{Dr}$

Link E:
- d: link length/2
- L_{ec} : length of center of mass
- M_E : mass of link

And let $S_1, S_2, S_3, C_1, C_2, C_3, S_{23}$ and C_{23} denote $\sin\theta_1$, $\sin\theta_2$, $\sin\theta_3$, $\cos\theta_1$, $\cos\theta_2$, $\cos\theta_3$, $\sin(\theta_2-\theta_3)$ and $\cos(\theta_2-\theta_3)$ respectively, then elements of dynamics equation are obtained as follows.

$$\begin{aligned}
M_{11} &= (L_1C_3 + L_{ac}C_2)^2 M_A + (d^2 + (L_2C_2 + L_{bc}C_3)^2)M_B \\
&\quad + (d^2 + L_{cc}{}^2C_3{}^2)M_C + (d^2 + L_{dc}{}^2C_2{}^2)M_D + I_{yyA}S_2{}^2 + I_{zzA}C_2{}^2 \\
&\quad + I_{yyB}S_3{}^2 + I_{zzB}C_3{}^2 + I_{yyC}S_3{}^2 + I_{zzC}C_3{}^2 + I_{yyD}S_2{}^2 \\
&\quad + I_{zzD}C_2{}^2 + I_{zzE} \\
M_{12} &= -dL_2M_BS_2 - dL_{dc}M_DS_2 \qquad (2) \\
M_{13} &= -dL_{bc}M_BS_3 + dL_{cc}M_CS_3 \\
M_{21} &= M_{12} \\
M_{22} &= M_AL_{cc}{}^2 + M_BL_2{}^2 + M_DL_{dc}{}^2 + I_{xxA} + I_{xxD} \\
M_{23} &= L_1L_{ac}M_AC_{23} + L_2L_{bc}M_BC_{23} \\
M_{31} &= M_{13} \\
M_{32} &= M_{23} \\
M_{33} &= M_AL_1{}^2 + M_BL_{bc}{}^2 + M_CL_{cc}{}^2 + I_{xxB} + I_{xxC}
\end{aligned}$$

$$\begin{aligned}
C_{11} &= (-(L_1C_3 + L_{ac}C_2)L_{ac}M_AS_2 - (L_2C_2 + L_{bc}C_3)L_2M_BS_2 \\
&\quad - L_{dc}{}^2M_DC_2S_2 + I_{yyA}C_2S_2 - I_{zzA}C_2S_2 + I_{yyD}C_2S_2 - I_{zzD}C_2S_2)\dot{\theta}_2 \\
&\quad + (-(L_1C_3 + L_{ac}C_2)L_1M_AS_3 - (L_2C_2 + L_{bc}C_3)L_{bc}M_BS_3 \\
&\quad - L_{cc}{}^2M_CC_3S_3 + I_{yyB}C_3S_3 - I_{zzB}C_3S_3 + I_{yyC}C_3S_3 - I_{zzC}C_3S_3)\dot{\theta}_3 \\
C_{12} &= (-(L_1C_3 + L_{ac}C_2)L_{ac}M_AS_2 - (L_2C_2 + L_{bc}C_3)L_2M_BS_2 \\
&\quad - L_{dc}{}^2M_DC_2S_2 + I_{yyA}C_2S_2 - I_{zzA}C_2S_2 + I_{yyD}C_2S_2 - I_{zzD}C_2S_2)\dot{\theta}_1 \\
&\quad + (-dL_2M_BC_2 - dL_{dc}M_DC_2)\dot{\theta}_2 \\
C_{13} &= (-(L_1C_3 + L_{ac}C_2)L_1M_AS_3 - (L_2C_2 + L_{bc}C_3)L_{bc}M_BS_3 \\
&\quad - L_{cc}{}^2M_CC_3S_3 + I_{yyB}C_3S_3 - I_{zzB}C_3S_3 + I_{yyC}C_3S_3 - I_{zzC}C_3S_3)\dot{\theta}_1 \\
&\quad + (-dL_{bc}M_BC_3 + dL_{cc}M_CC_3)\dot{\theta}_3 \\
C_{21} &= ((L_1C_3 + L_{ac}C_2)L_{ac}M_AS_2 + (L_2C_2 + L_{bc}C_3)L_2M_BS_2 + L_{dc}{}^2M_DC_2S_2 \\
&\quad - I_{yyA}C_2S_2 + I_{zzA}C_2S_2 - I_{yyD}C_2S_2 - I_{zzD}C_2S_2)\dot{\theta}_1 \\
C_{22} &= 0 \\
C_{23} &= (L_1L_{ac}M_AS_{23} + L_2L_{bc}M_BS_{23})\dot{\theta}_3 \\
C_{31} &= (-(L_1C_3 + L_{ac}C_2)L_1M_AS_3 - (L_2C_2 + L_{bc}C_3)L_{bc}M_BS_3 - L_{cc}{}^2M_CC_3S_3 \\
&\quad + I_{yyB}C_3S_3 - I_{zzB}C_3S_3 + I_{yyC}C_3S_3 - I_{zzC}C_3S_3)\dot{\theta}_1 \\
C_{32} &= (-M_AL_{ac}L_1S_2C_3 + M_AL_{ac}L_1C_2S_3 - \frac{1}{2}M_BL_1L_2C_3S_2 + \frac{1}{2}M_BL_1L_2C_2S_3)\dot{\theta}_2 \\
C_{33} &= 0
\end{aligned}$$

$$\begin{aligned}
N_1 &= 0 \\
N_2 &= (M_AL_{ac} + M_BL_2 + M_DL_{dc})gC_2 \\
N_3 &= (M_AL_1 + M_BL_{bc} + M_CL_{cc})gC_3
\end{aligned}$$

2.3 Controller hardware design

A controller for proposed haptic device was also developed and specification of controller is listed in Table 1. Control hardware is implemented with floating point DSP to calculate dynamics as fast as 1ms.

Table 1 Specification of controller

	Specification
CPU	Floating point DSP, 150MHz
PC Interface	PC Parallel port
Input	- 3 Channel rotary incremental encoder interface - 2 bit sequence signal input
Output	- 3 Channel motor drive output (up to 5A per channel) - 2 bit sequence signal output

3. DYNAMIC COMPENSATOR

In this section, we build a dynamic compensator. Let F denote desired output force, then actuator torque is give by

$$\tau = J^T F \tag{3}$$

Where, J is Jacobian matrix and given as follows.

$$J = \begin{pmatrix} -L_1C_1C_3 - L_3C_1C_2 & L_3S_1S_2 & L_1S_1S_3 \\ -L_1S_1C_3 - L_3S_1C_2 & -L_3C_1S_2 & -L_1C_1S_3 \\ 0 & L_3C_2 & L_1C_3 \end{pmatrix} \tag{4}$$

Even though each actuator generates torque τ, we can't get output force F exactly, because of load torque such as gravity force, friction and inertia. If we control haptic device with open loop control scheme, we need to compensate them to get exact force. Gravity force N is a function of position, and friction torque $\tau_{friction}$, which appears in [8] is a function of angular velocity. If we ignore Coriolis force, parasitic force which is due to dynamics is given as follows, where M is inertia matrix.

$$\tau_M = M\ddot{\theta} \tag{5}$$

Then torque τ_{comp} to compensate parasitic force is given as:

$$\tau_{comp} = N + \tau_{friction} + \tau_M \tag{6}$$

Actual torque τ_{cmd} that actuator must produce to get output force F is

$$\tau_{cmd} = \tau_{comp} + \tau \tag{7}$$

And amplitude of current of each servo amplifier, I_{cmd} is

$$I_{cmd} = K^{-1} \cdot G^{-1} \cdot \tau_{cmd} \tag{8}$$

K : torque constant matrix

G : Gear ratio matrix

For proposed haptic device, K is given by diag(0.0603, 0.0603, 0.0603) and G is given by diag(10.0, 10.7,10.7). Fig. 3 shows block diagram of control system. $\dot{\theta}$ and $\ddot{\theta}$ are obtained by low pass filtering after differentiating $\theta, \dot{\theta}$ respectively.

4. EXPERIMENTAL RESULT

4.1 Performance evaluation of proposed haptic device

In this section, we evaluate the performance of developed haptic device which is shown in Fig. 4. There are many indices to evaluate the performance of a haptic device. In this paper, we select the size of workspace, maximum force, force response bandwidth and force resolution as indices. Figure 5 shows workspace, which is as large as 60cm x 30cm x 80cm.

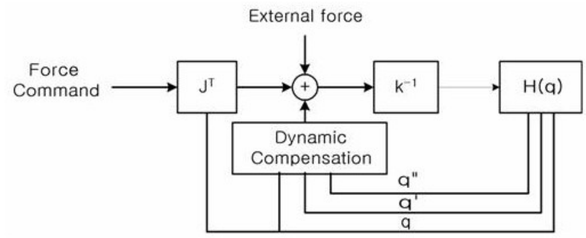

Fig. 3 Block diagram of control system

(a) Haptic device

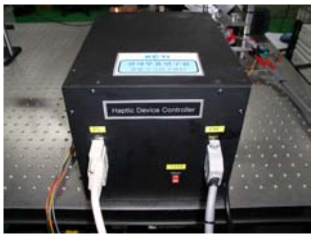

(b) Controller

Fig. 4 Portrait of developed haptic device and controller

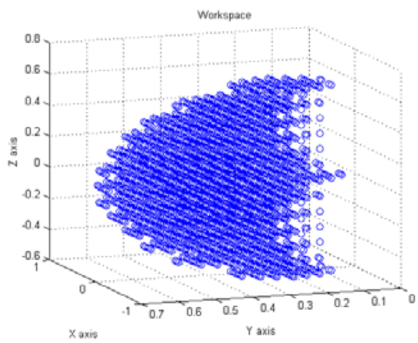

Fig. 5 Workspace of developed haptic device (Numerical result)

Maximum continuous force at the point where proposed haptic device produces maximum force is as high as 14N, which is quite larger than that of PHANToM series. Fig 6 shows continuous maximum force in X axis. If force command exceeds some level, output force does not increase, because motor currents are saturated. In Y and Z direction, output force decreases if it exceeds maximum force, because axis 2, 3 are driven differentially. At the point where the manipulability becomes maximum and operator is supposed to work, we obtain continuous maximum force 5~6N in each direction.

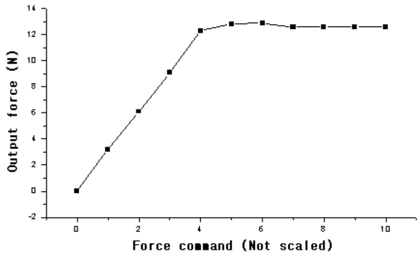

Fig. 6 Maximum continuous output force (X direction)

Force response bandwidth which is the maximum frequency that a haptic device can follow the force command without attenuating its amplitude more that 3dB. It is an important performance index because human are sensitive to change of force rather than absolute amplitude of force. We obtained 70Hz as seen in Fig. 7.

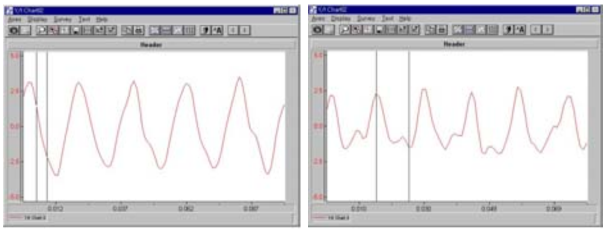

(a) (b)
Fig. 7 Force response, (a) 50Hz, (b) 70Hz (Y direction)

Finally, as seen in Fig 8, force resolution is about 0.007N.

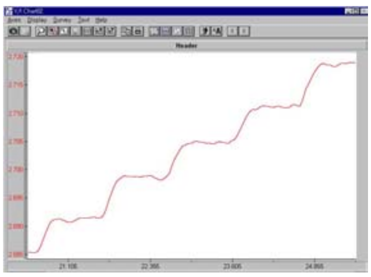

Fig. 8 Small step force command versus output force (unit N, Y direction)

4.2 Dynamics compensation experiments

Test bed to measure parasitic force consists of a linear stage, haptic device, force sensor and DAQ system as shown in Fig. 9. Linear stage moves hand of haptic device in X direction. Hand is connected to linear stage by a universal joint and a force sensor. Linear stage accelerates by $5m/s^2$ from stop position until velocity reaches 5cm/s and moves with constant speed after that. Force is measured at the hand of haptic device.

Fig. 10-(a) shows measured force with no compensation control scheme. Maximum force which is due to system dynamics is approximately 1.5N. Tail of graph is due to Coulomb friction force and its amplitude is about 0.8N. Fig. 10-(b) is a result when we add dynamics compensator. Maximum force is about 1.0N, which is smaller by 0.5N than that of (a) but Coulomb friction force remains same. Fig. 10-(c) shows measured force with additional Coulomb friction compensator. Force measured at the tail decreased to 0.4N, which is nearly half of (a), but unexpected ringing occurred. We think it comes from speed and acceleration measurement delay.

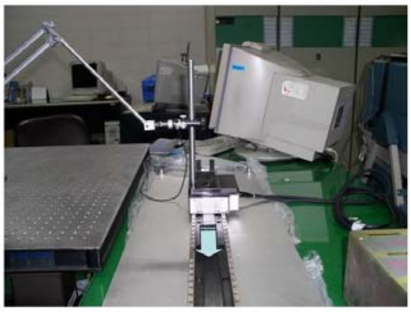

Fig. 9 Test bed for dynamics compensation

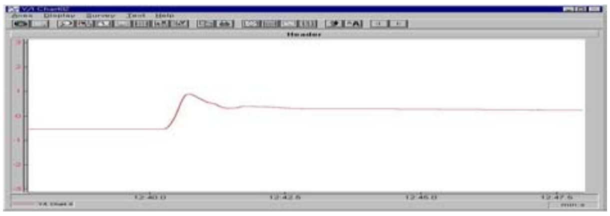

(a) No compensation

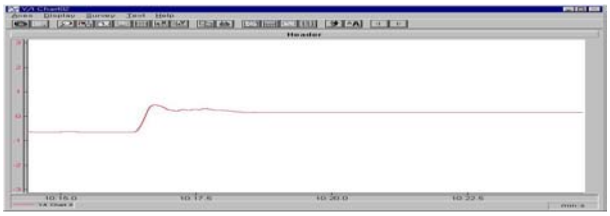

(b) Dynamics compensation

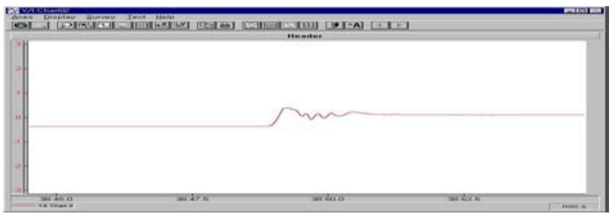

(c) Dynamic and Coulomb friction compensation

Fig. 10 Measured parasitic force

5. CONCLUSION

We presented a new five-link type 3DOF haptic device which has simple dynamics so that we can easily model its dynamics and compensate effect of dynamics. To reduce the effect of dynamics, we located all DC motors on base frame and actuator torque was transferred by wire and wheel. We evaluated its performance with some performance indices like volume of workspace, maximum force, force response bandwidth, and force resolution. Maximum continuous force reached to 14N and workspace was as large as 60cm x 30cm x

80cm. Force command bandwidth was 70Hz and force resolution was 0.007N. So we think this device is suitable for general purpose haptic device. We also proposed dynamic compensation method and presented an experimental result. An experimental result showed parasitic force which was due to device dynamics and friction decreased by 50%. We need to implement new test bed with 3D Cartesian robot instead of linear stage to measure 3D force to measure 3-directional parasite force. As a future work, we plan to implement a coarse-fine type haptic system to display vibration information with developed haptic device.

REFERENCES

[1] Robert J. Anderson, Mark W. Spong, "Bilateral control of teleoperators with time delay", *IEEE Trans. On Automatic Control*, Vol. 34, No. 5, pp. 494-501, 1989

[2] Sun-Gi Hong, Ju-Jang Lee, and Seungho Kim, "Generating artificial force for feedback control of teleoperated mobile robots", *Proc. of IEEE/RSJ International Conf. on Int. Robot & Sys.*, pp. 1721-1726, 1999

[3] Sokho Chang, Jungtae Kim, Insup Kim, Jin Hwan Borm , and Chongwon Lee, "KIST Teleoperation system for humanoid robot", *Proc. of IEEE/RSJ International Conf. on Int. Robot & Sys.*, pp. 1198-1203, 1999

[4] Metin Sitti, Baris Aruk, Hiroaki Shintani, and Hideki Hashimoto, "Development of a scaled teleoperation system for nano scale interaction and manipulation", *Proc. of International Conf. on Robotics and Automation,* pp. 860-867, 2001

[5] Andreas O. Frank, I. Alexander Twombly, Timothy J. Barth and Jeffrey D. Smith, "Finite element methods for real-time haptic feedback of soft-tissue models in virtual reality simulators", *Virtual Reality, Proc. IEEE* , pp. 257-263, 2001

[6] Dae Hyun Kim, Nak Yong Ko, Geum Kun Oh, and Young Dong Kim, "A framework for haptic rendering system using 6-DOF force-feedback device", *Proc. of International Conf. on Robotics and Automation*, pp.874-879, 2001

[7] B. J. Unger, A. Nicolaidis, P. J. Berkelman, A. Thompson, R. L. Klatzky, and R. L. Hollis, "Comparison of 3-D haptic peg-in-hole tasks in real and virtual environments" , *Proc. of IEEE/RSJ International Conf. on Int. Robot & Sys.*, pp. 1751-1756, 2001

[8] Dong-Soo Kwon, and Ki Young Woo, "Control of the Haptic Interface with Friction Compensation and Its Performance evaluation", *Proc. of IEEE/RSJ International Conf. on Int. Robot & Sys.*, pp. 955-960, 2000

[9] David T. Burns, "Design of a six degree of freedom haptic interface", Master Thesis, Northwester University, 1996